FAULT GEOMETRY AND ASEISMIC SLIP ON THE SOUTHERN SAN ANDREAS FAULT, CALIFORNIA

Abstract

Recent fractures of the southern San Andreas fault in the Coachella Valley form a sawtooth geometry consisting of five 7-14Km long segments that alternate in trend from N40W to N48W. The relationship between this simple geometry and the inferred plate slip vector (N40W) is responsible for the topographic features of the fault zone, for the spatial distribution of triggered slip in 1968 and 1979 and for active uplift near the fault zone. The study of strainfields surrounding the oblique slipping N48W segments may provide clues concerning the rupture of the southern San Andreas in a future major earthquake.

The southern San Andreas Fault from the Cajon Pass to the Salton Sea is a seismic gap. It has not experienced a major earthquake in historic time (>240 years) and adjoins the rupture zones of major historic earthquakes to the north (1857 Fort Tejon), and to the south (1915, 1940 and 1979 Imperial Valley earthquakes). It is characterized by an almost total absence of microseismicity. A possible magnitude for a future earthquake on this segment of the fault has been estimated to be $7.6<M_w<7.8$ with a recurrence interval of between 160 and 360 years. [1] Holocene fault activity has resulted in clear topographic expression of the fault in numerous locations. [2-5] Trilateration in the last decade[6,7] and triangulation since 1931 [8] reveal 25mm/a of dextral displacement across the Coachella Valley. Prehistoric movements of the fault are evident in trench studies across the fault at Indio and at Cajon Pass [9]. Ongoing aseismic slip on the fault[10] may be responsible for the pronounced topographic features of the mapped fault, especially where Lake Cahuilla sediments should have obliterated transient features in the last several hundred years.[5,10,11]

On most fault maps of California the Coachella Valley section of the San Andreas fault south of the Banning Fault is shown as an approximately straight line. Careful mapping of recent fault features[5] reveals three N48W linear segments separated by N43W and N40W segments (Figure 1). Recent fault features are found within 50m of these linear trending segments except for the northern end of the central N48W segment and the southern end of the south N48W segment, where the deviation from straightness locally exceeds 100m. The 7-14Km dimensions of the fault segments form significant structural elements extending perhaps to the seismogenic zone as proposed by Wallace[12] in central California. The North-American/Pacific plate slip vector is estimated[13] to be locally parallel to N40W which would result in approximately pure shear along the N43W and N40W segments of the fault and oblique slip on the N48W segments. The oblique slip gives rise to transpressive folding[3] on segments forming the Indio Hills[4], Mecca Hills[3] and Durmid Anticline.[2]

Part of the southern San Andreas fault slipped soon after the Borrego Mountain and Imperial Valley earthquakes in 1968 and 1979. The process was described[11] as "triggered-slip" because aseismic dextral movements of the fault occurred at the time of, and shortly after, nearby seismic events. Puzzling features of this aseismic triggered-slip were the small amplitudes (1-20mm) of dextral displacements (Figure 2) that occurred along a 40Km long section of the fault, the much reduced slip in the central 13Km of the triggered section and the evident increase in slip from south to north that terminated abruptly without apparent cause.[11,14,15] The fault geometry reported in this article provides additional insight into the mechanism of triggered slip. The triggered section embraces the three southern segments defining the saw-tooth geometry of the fault. Major bends in the fault zone occur within 2Km of the ends of the northern triggered-slip section and within 4Km of the southern triggered section in 1979. The N40W segment corresponds to the zone where no slip was observed 1979 and where 6-8mm of slip was observed on a 500m long surface break in 1968.[15]

An apparent paradox exists. Triggered-slip is confined to the oblique slip segments of the fault where normal forces inhibiting slip are large[15] and is insignificant on the pure shear segments where slip may be anticipated to occur more readily. A possible mechanism is that the N40W segments are creeping uniformly with time and that the N48W segments are "pinned". A similar scheme has been invoked[17] to describe the nature of seismic slip on the San Andreas in central California. Data from leveling surveys in 1974 and 1978 confirm that part of the Durmid Anticline segment is actively deforming[2] and that the observed bulge coincides approximately with the 1979 southern triggered segment. Evidence for continuous creep in the N40W and N43W segments is more elusive since most of the data for fault creep have been acquired on the N48W fault segments where the fault is well-expressed. A creep rate of 2mm/a is present at Dillon Road close to the bend between the northern N48W and the N43W segment[18].

Indirect evidence for creep in the N40W segment near North Shore exists as damage to a 36 year old, 5Km long, North-South concrete drain known as Wasteway No.1 that extends from the Coachella Canal to the northermost shore of the Salton Sea (Figure 1). Compressional cracks in the concrete and deformed reinforcing bars are found in two clusters; a pair of northern fractures within 500m of the interpolated intersection of the fault with the wasteway and a sequence of five southern fractures 2Km SW of the fault induced by hydraulic forces[19]. An apparent shortening by

50±10mm in the northern two fractures appears to be the result of tectonic movements in the last 36 years. The southern of the two northernmost fractures exhibits greater damage to the eastern lip of the structure consistent with clockwise rotation of the wasteway to the north by right lateral shear. If the fractures are the result of dextral slip on the fault, a value of 1.8±0.4mm/a is indicated, a creep rate that is intermediate between slip monitored on adjacent N48W segments[18].

A subsurface survey using an impulse radar profiling system was conducted along the west side of the wasteway and in a number of nearby locations to determine the precise intersection of the fault with the wasteway. These data reveal an abundance of possible fractures that appear to have disturbed the 1-2m deep Cahuilla Lake beds (Figure 2). The disturbances evident in the sediments occur over a 1Km wide zone and are not restricted to where thrust joints in the wasteway are located. They diminish in frequency and complexity in the southern half of the wasteway. The fault zone is perhaps wider in this segment than in adjacent segments and it is therefore possible that distributed slip could occur without causing ground cracks. The absence of recorded creep on the North Shore creepmeter (within the N40W segment) and the approximately 1mm/a measured on the nearby geodetic array[18] suggest that creep may be occurring either on a fault strand other than one on which cracks occurred in 1968 or that creep is distributed over a wide shear zone.

We note that the mean of the maximum values of triggered-slip measured in each kilometer section of the fault in 1968 (14.5mm) is roughly twice that observed in 1979 (6.5mm). Earthquakes capable of generating comparable accelerations to those that triggered the fault in 1968 and 1979 occurred in 1940 (El Centro), 1942 (San Jacinto) and 1948 (Desert Hot Springs). The period of time between the most recent of these and 1968 is twice as long as the interval between 1968 and 1979. A slip-predictable model for triggered-slip may be applicable in which the magnitude of triggered slip is proportional to the time since previous triggered slip occurred. No slip was recorded on the southern San Andreas in the 1940's nor was evidence for it sought. Aperiodic creep on the fault in the Coachella Valley and triggered-slip appear to be manifestations of the same phenomenon. The creep rate following triggered-slip in these segments is typically lower than at other times[18]. Similar accelerated creep (0.1-8.7mm) was triggered on the San Andreas fault in central California at the time of the Coalinga earthquake.[22]

Leveling data from the NW end of the southern N48W segment indicate a tilt rate up to the east of the order of 1 microradian/a in the period 1980-83 [20], followed in April 1984 by an 8mmm creep event at Mecca Beach.[18] NGS Leveling data reveal a similar tilt rate to have occurred in 1974-78 (Figure 1) close to part of the triggered slip segment of 1979. If this uplift (≈3mm/a) were entirely due to vertical strains induced by horizontal compressional confinement of a 15Km thick crust, we calculate a horizontal strain rate of -0.6 microstrain/a, assuming a Poisson's ratio of 0.25 in the elastic zone centered on the fault. The width of the zone of folding near the fault is of the order of 5Km which suggests that the observed uplift requires convergence of the order of 3mm/a outside the zone of folding. This figure is consistent with the observed long term creep rate and confirms that elastic strain must be accumulating away from the fault, since this represents less than 20% of the dextral displacement observed geodetically across the Coachella Valley. USGS trilateration at Bat Caves Buttes mostly to the north of the fault and 3Km from the SE termination of triggered-slip (outside the uplift zone) indicates that no deformation has occurred (±1 microstrain) in the last decade [21].

The association of N48W trending segments of the fault with high ground, well-developed fault features, thrusting and folding is in marked contrast to the poor surface expression, subdued topography and low elevation of the fault to be found in the N40W and N43W segments. The absence of topographic relief in direct line with the southernmost expression of the San Andreas Fault SE of the Salton Sea supports the hypothesis that the trend of the active southern continuation of the San Andreas is less than N48W, perhaps passing through Bombay Beach [10]. The swarm of seismic activity on the Brawley fault zone [24] preceeding the Imperial Valley 1979 event trends at N22±2W and may represent the effective continuation of the San Andreas Fault southward. The observed elevation changes near the Salton Sea in 1974-8 were presumably related to the Brawley earthquake swarm.

Angular relationships between adjacent linear segments of the San Andreas fault have recently been discussed in terms of their influence in the control of strain release during late stages of the earthquake cycle.[16,17] King and Nabelek[23] demonstrate the generality of such observations and provide a kinematic mechanism for the nucleation and termination of slip at bends in faults. The possibility exists that each of the N48W segments on the San Andreas, or the Banning fault, could act as a nucleus for rupture of the southern San Andreas. The geometry and slip vector associated with this 90Km segment of the fault are well determined. Strainfields will be most intense at the ends of the mapped straight segments[16], generally requiring networks with baselines of less than a few kilometers, extending tens of kilometers from the fault. Existing trilateration and leveling networks are inappropriately scaled and poorly distributed to monitor these strainfields. It is of great importance to establish a few key networks in strategically placed locations if we are to learn more about the rupture process in the Coachella Valley.

Roger Bilham

Lamont Doherty Geological Observatory, Palisades, N.Y. 10964. Current address, Joint Institute for Laboratory Astrophysics, University of Colorado, Boulder, CO, 80309

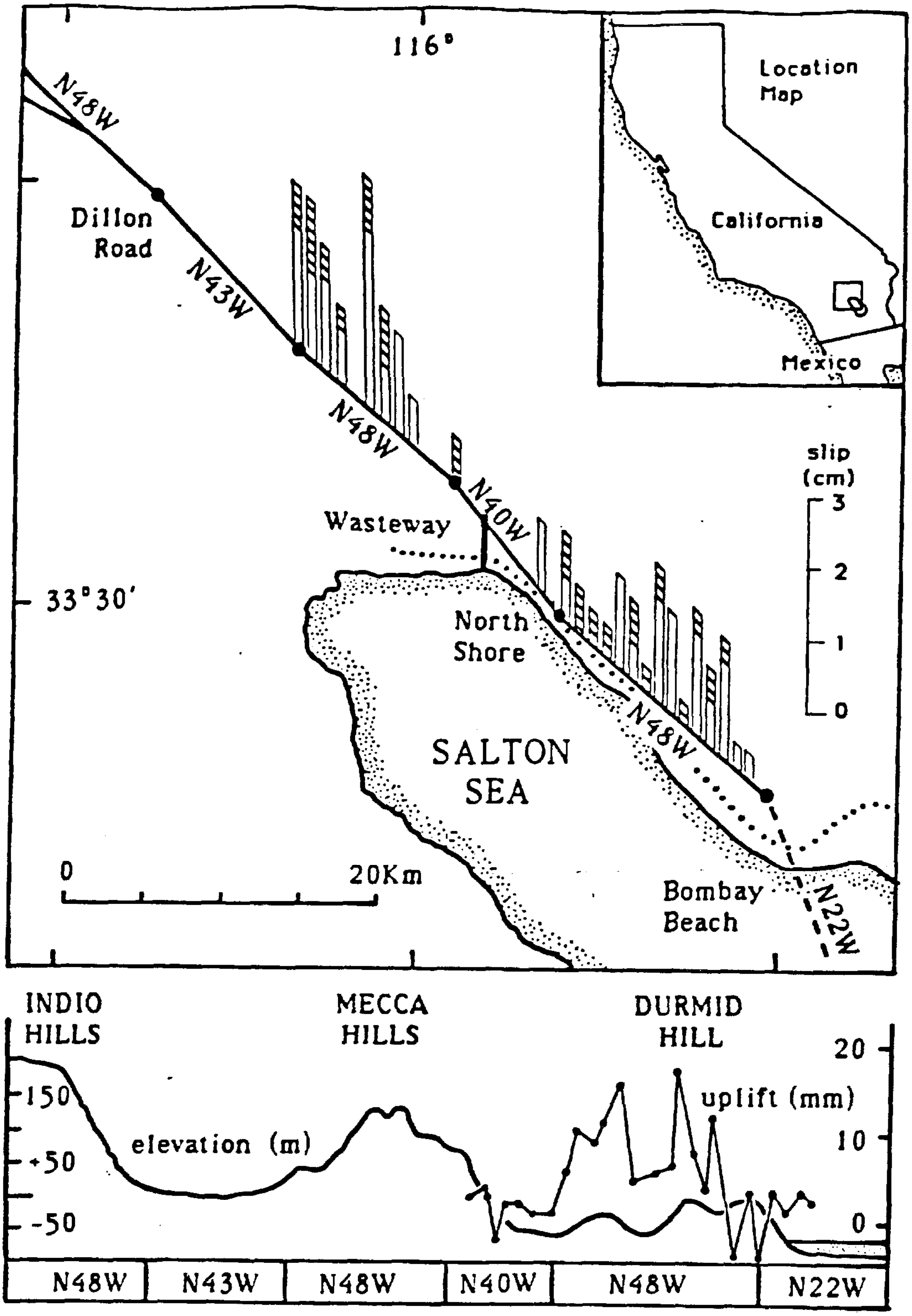

Figure 1 Coachella Valley section of the San Andreas fault from the intersection of the Banning Fault to the Brawley seismic swarm (dashed line). Recent fault features follow a series of 7-18Km long segments that are linear to ±50m but differ in trend by 3-8°. The cumulative, mean, maximum triggered-slip observed on the fault is shown for each kilometer of the fault (open bars=1968, striped bars=1979). Uplift observed on a leveling line near the fault (dotted line) between 1974 and 1978 is plotted on the lower figure which also shows the relationship between fault trend and fault-trace elevation. A North-South trend believed to be due to a magnetic bias in one of the surveys has been removed from the NGS leveling data.

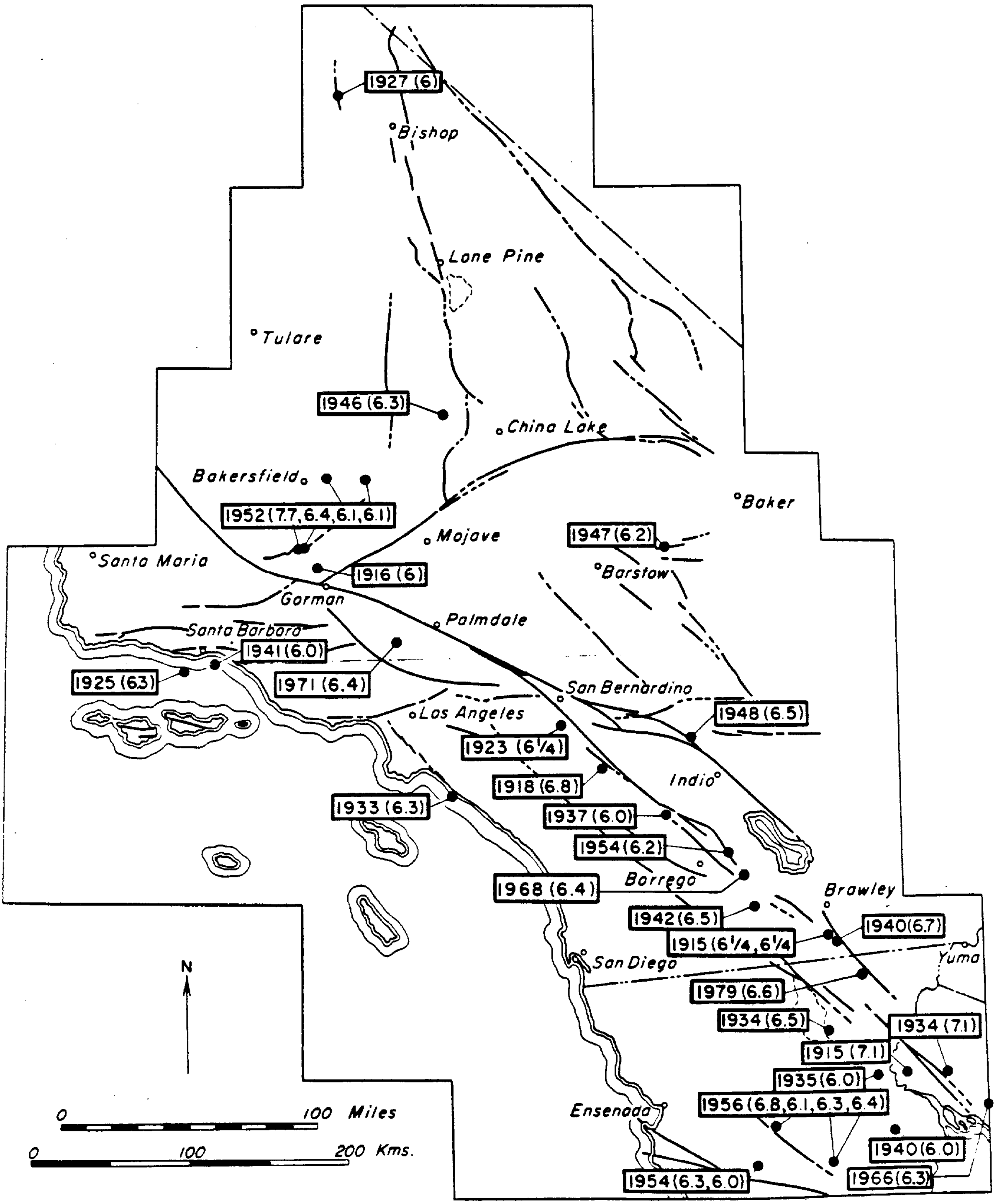
1927 (6)
Bishop
Lone Pine
Tulare
1946 (6.3)
China Lake
Bakersfield
1952 (7.7, 6.4, 6.1, 6.1)
Baker
Mojave
1947 (6.2)
Santa Maria
1916 (6)
Barstow
Gorman
Palmdale
Santa Barbara
1941 (6.0)
1925 (6.3)
1971 (6.4)
San Bernardino
Los Angeles
1948 (6.5)
1923 (6 1/4)
Indio
1918 (6.8)
1933 (6.3)
1937 (6.0)
1954 (6.2)
Borrego
1968 (6.4)
Brawley
1942 (6.5)
1940 (6.7)
1915 (6 1/4, 6 1/4)
Yuma
San Diego
1979 (6.6)
1934 (6.5)
1934 (7.1)
1915 (7.1)
1935 (6.0)
1956 (6.8, 6.1, 6.3, 6.4)
Ensenada
1940 (6.0)
1966 (6.3)
1954 (6.3, 6.0)
N
0
100 Miles
0
100
200 Kms.

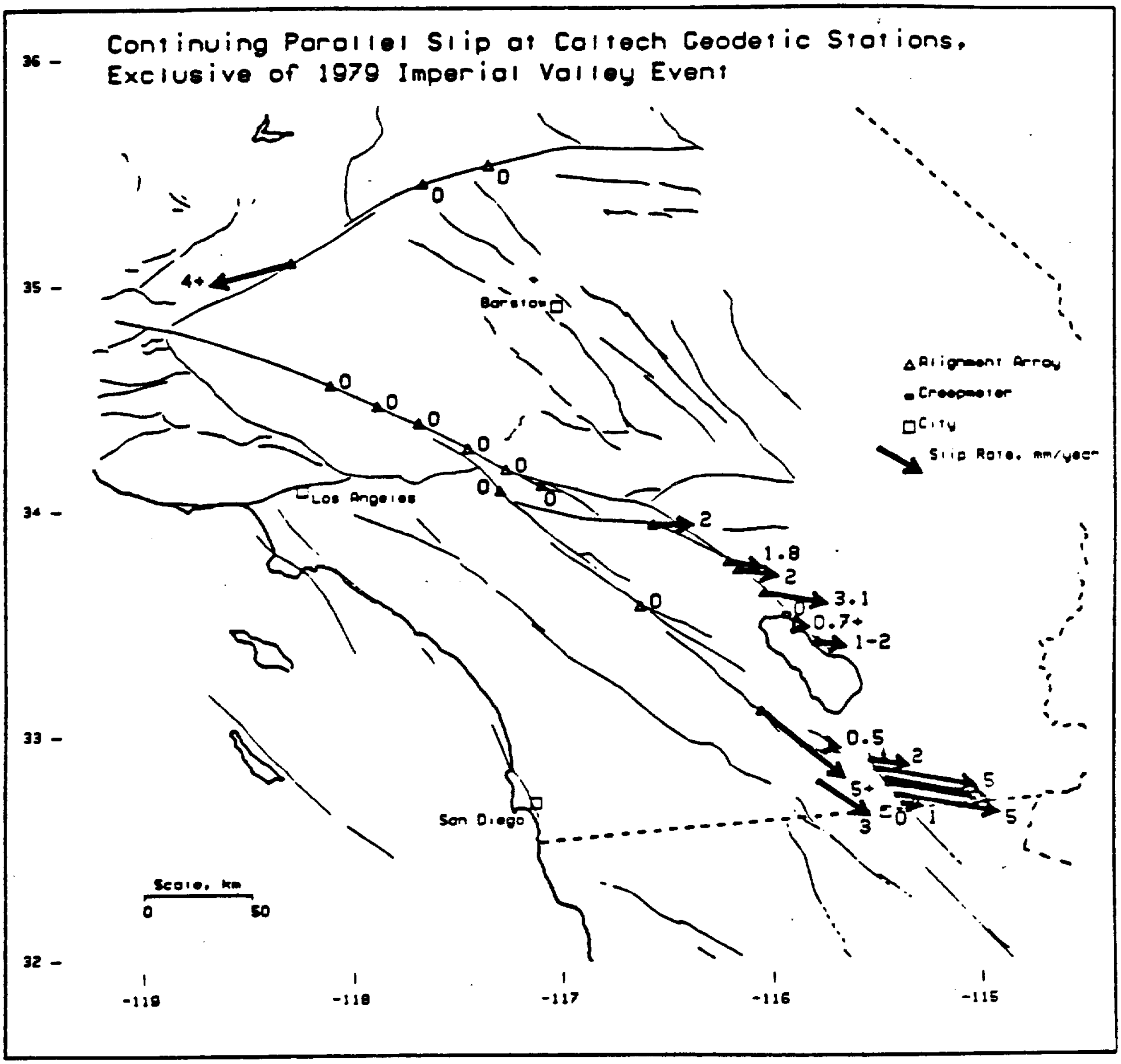

Figure 5.—Map summarizing observations in southern California of fault slip rates not associated with individual earthquakes showing surface rupture. All motion is assumed to be parallel to the fault traces; the arrows have lengths proportional to slip rates but are oriented only for pictorial purposes. Note the faults on which no slip has been measured.

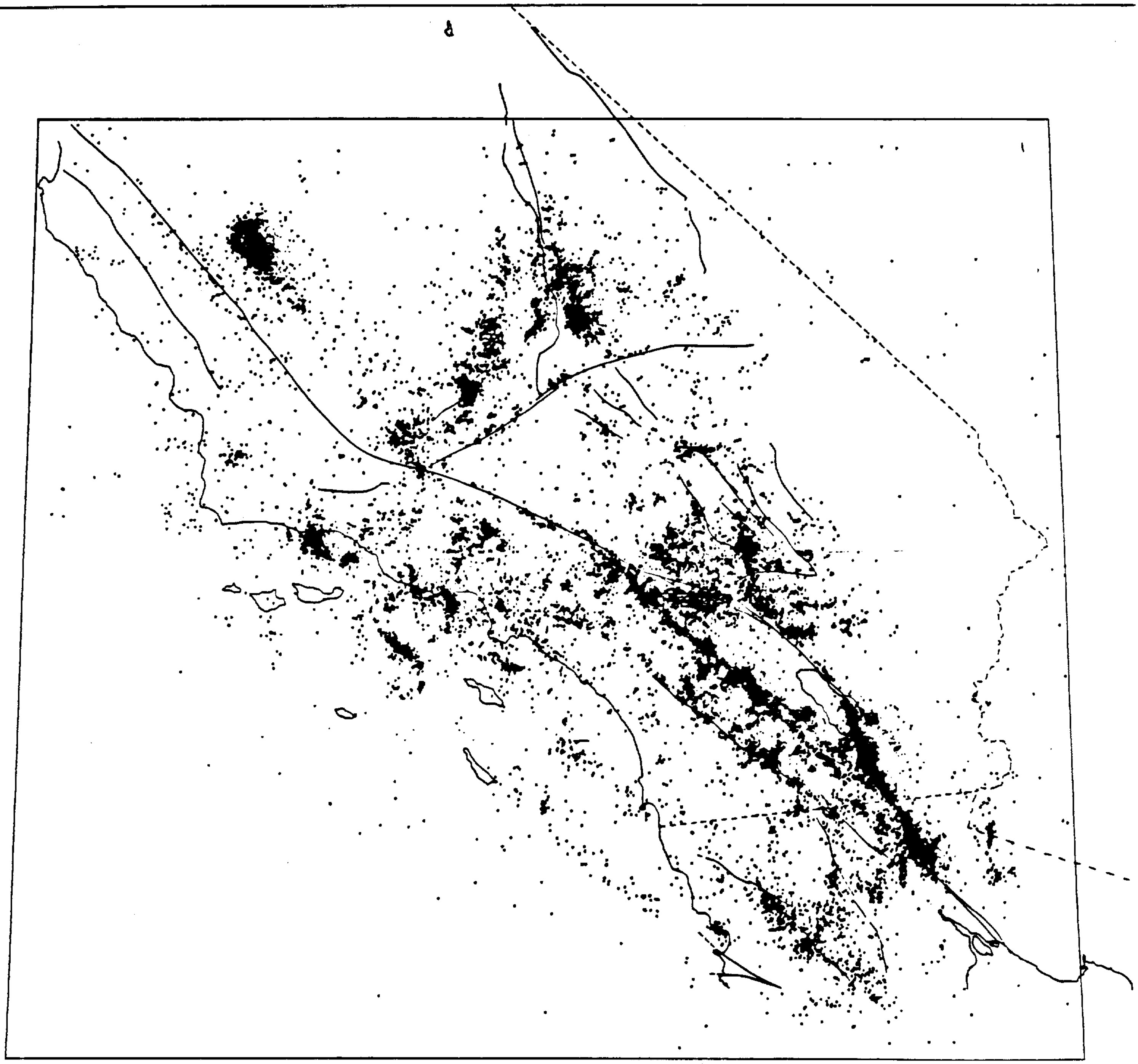

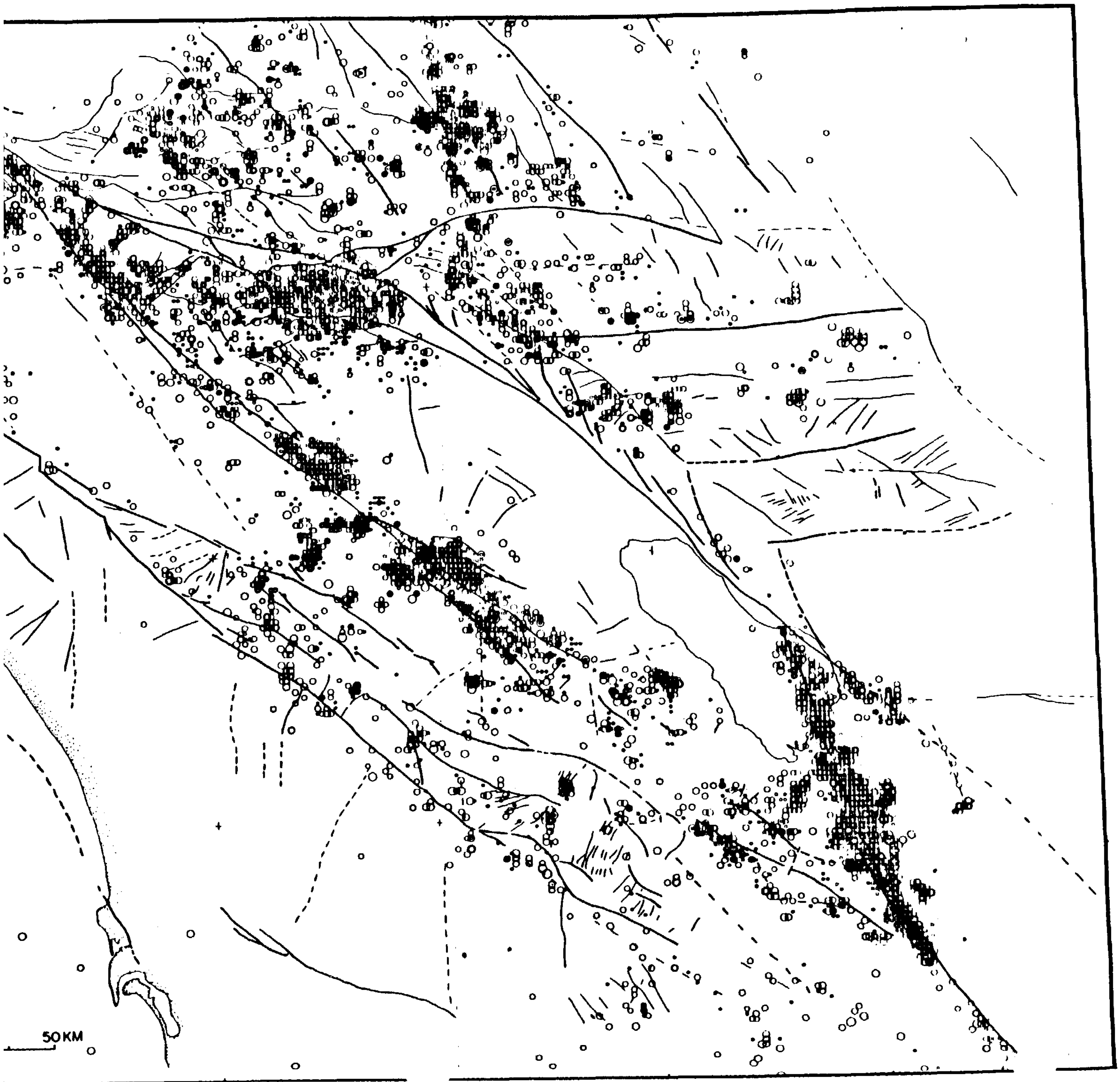
50 KM

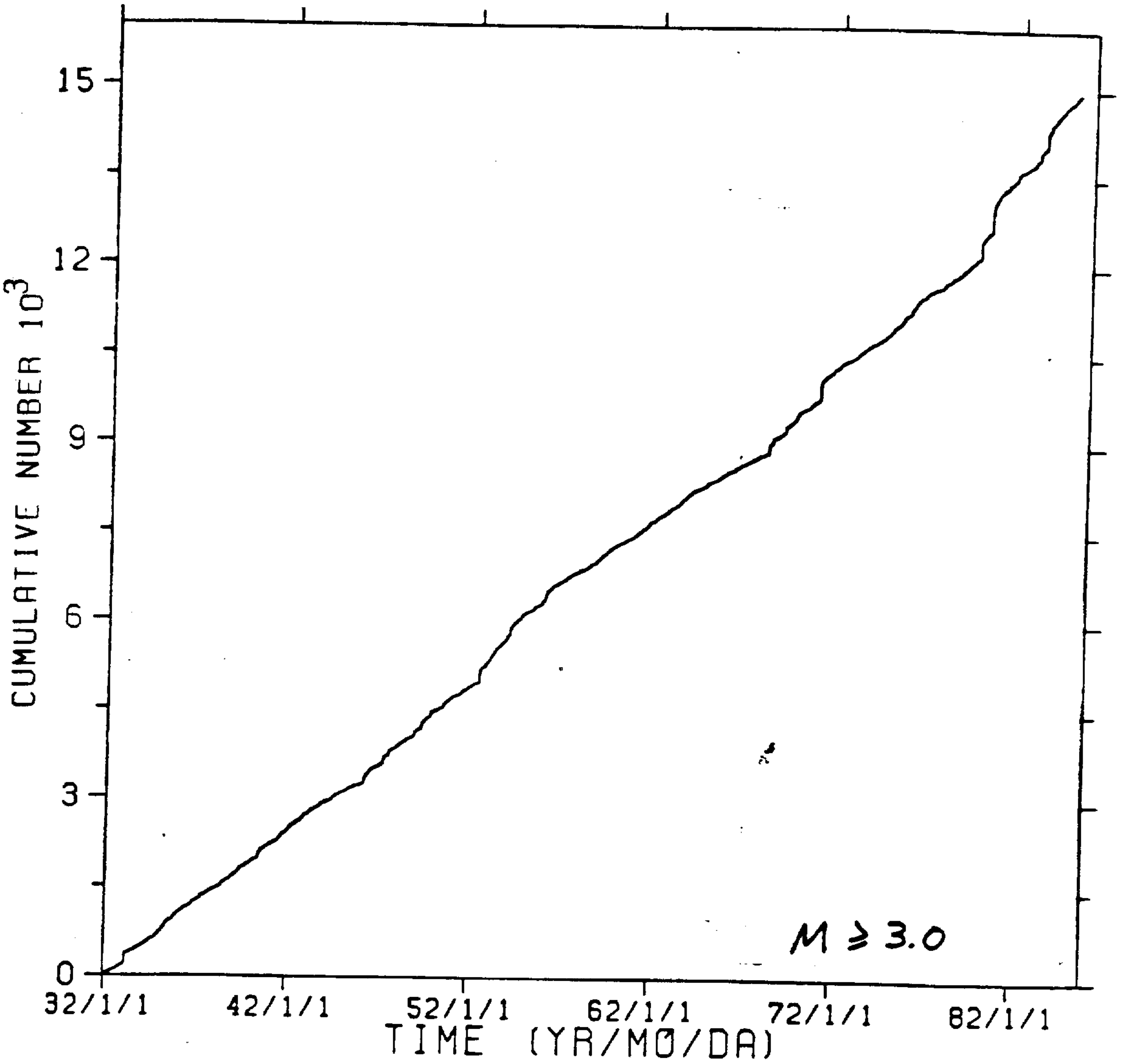
15
12
9
6
3
0
CUMULATIVE NUMBER 10^3
32/1/1
42/1/1
52/1/1
62/1/1
72/1/1
82/1/1
TIME (YR/MO/DA)
M ≥ 3.0

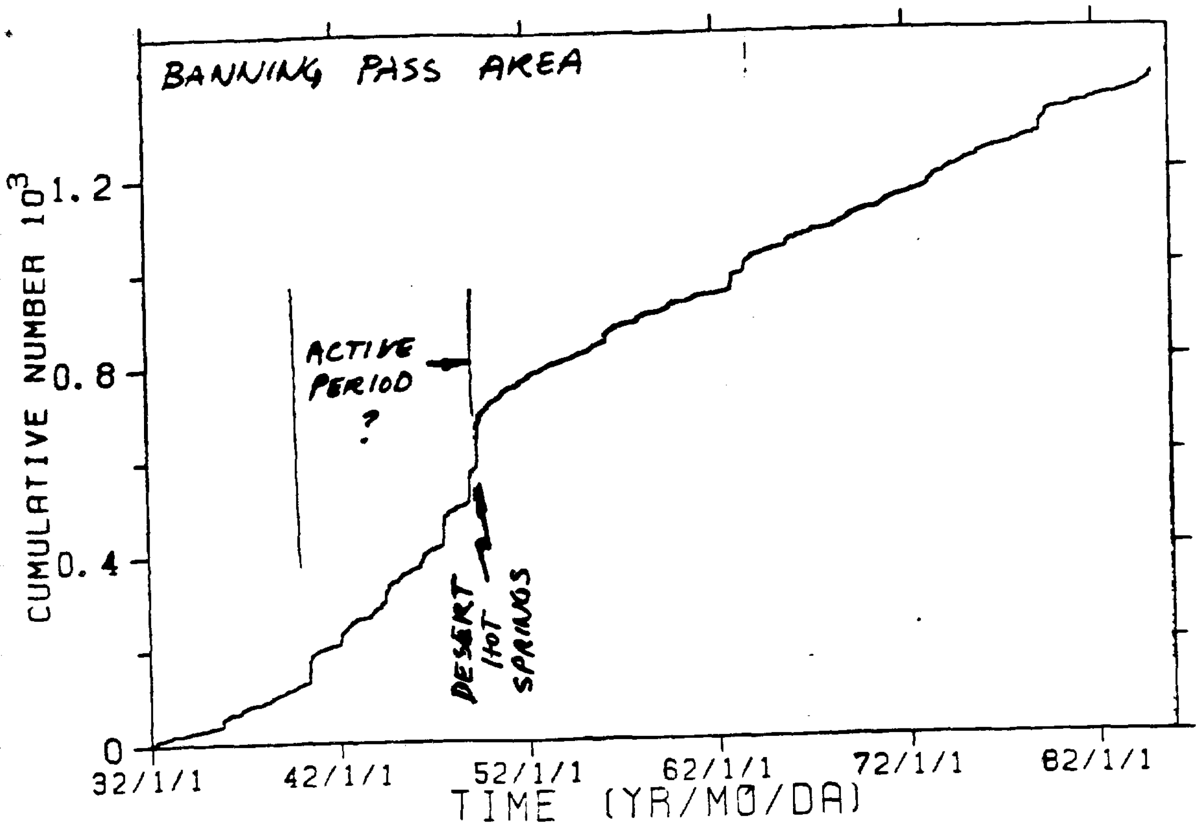
BANNING PASS AREA
ACTIVE PERIOD ?
DESERT HOT SPRINGS
CUMULATIVE NUMBER 10^3
0
0.4
0.8
1.2
32/1/1
42/1/1
52/1/1
62/1/1
72/1/1
82/1/1
TIME (YR/MO/DA)

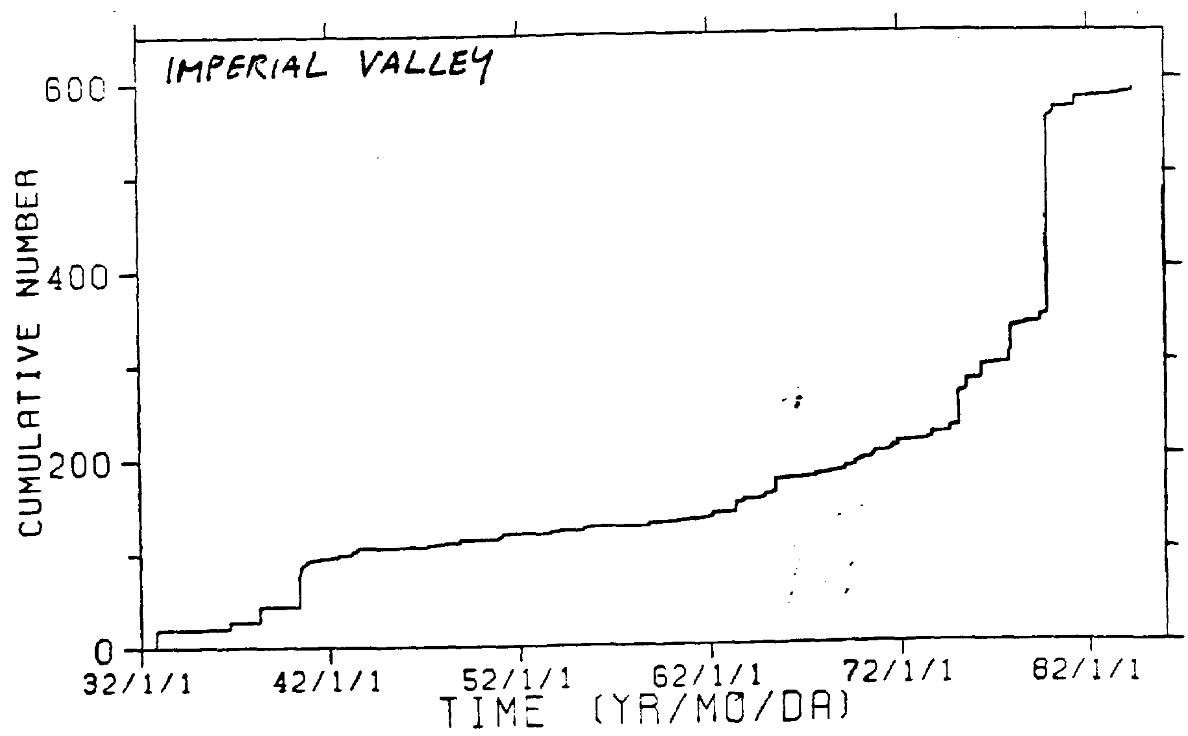
IMPERIAL VALLEY
CUMULATIVE NUMBER
0
200
400
600
32/1/1
42/1/1
52/1/1
62/1/1
72/1/1
82/1/1
TIME (YR/MO/DA)

1945 - 1954

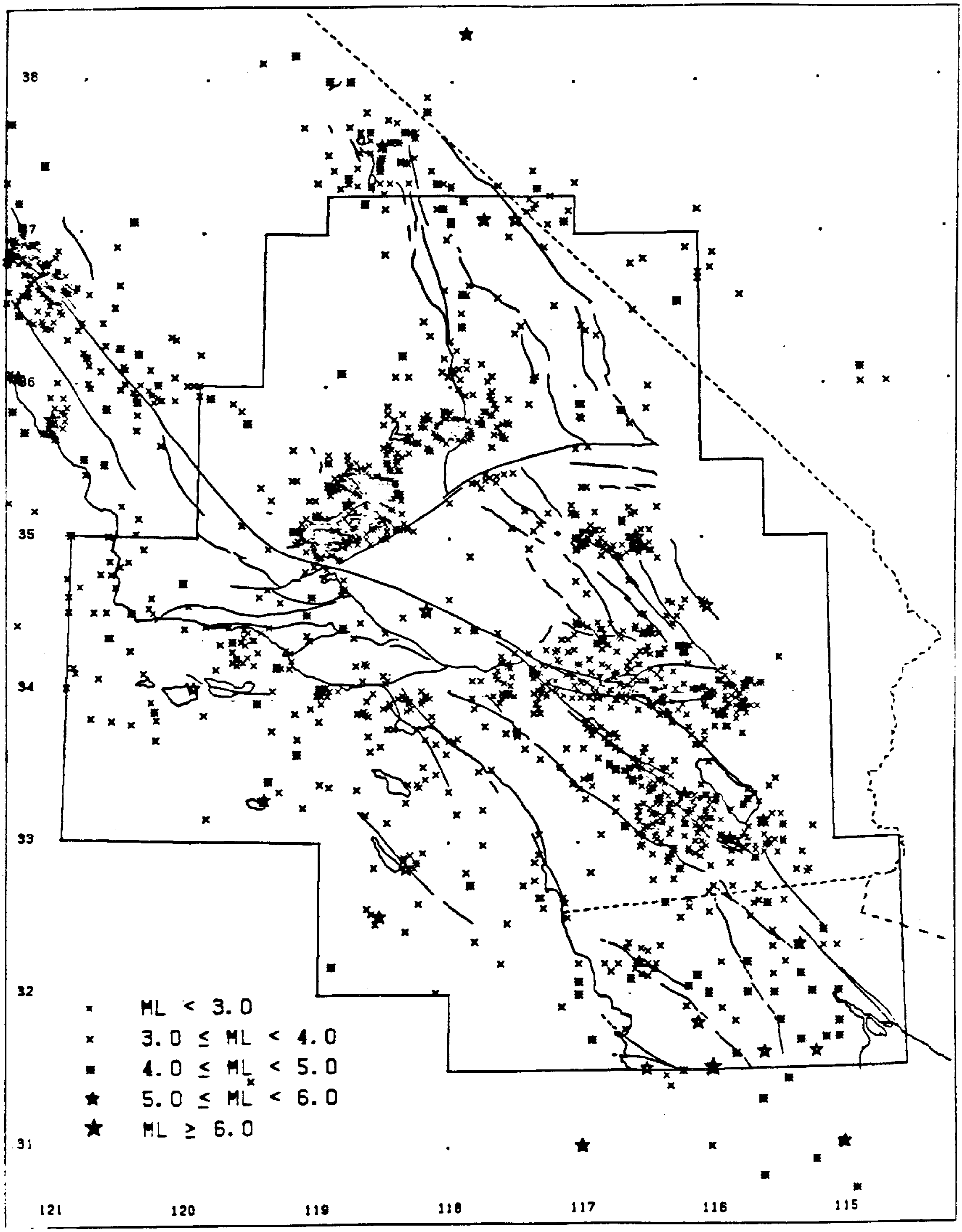
38
37
36
35
34
33
32
31
121
120
119
118
117
116
115
ML < 3.0
3.0 ≤ ML < 4.0
4.0 ≤ ML < 5.0
5.0 ≤ ML < 6.0
ML ≥ 6.0

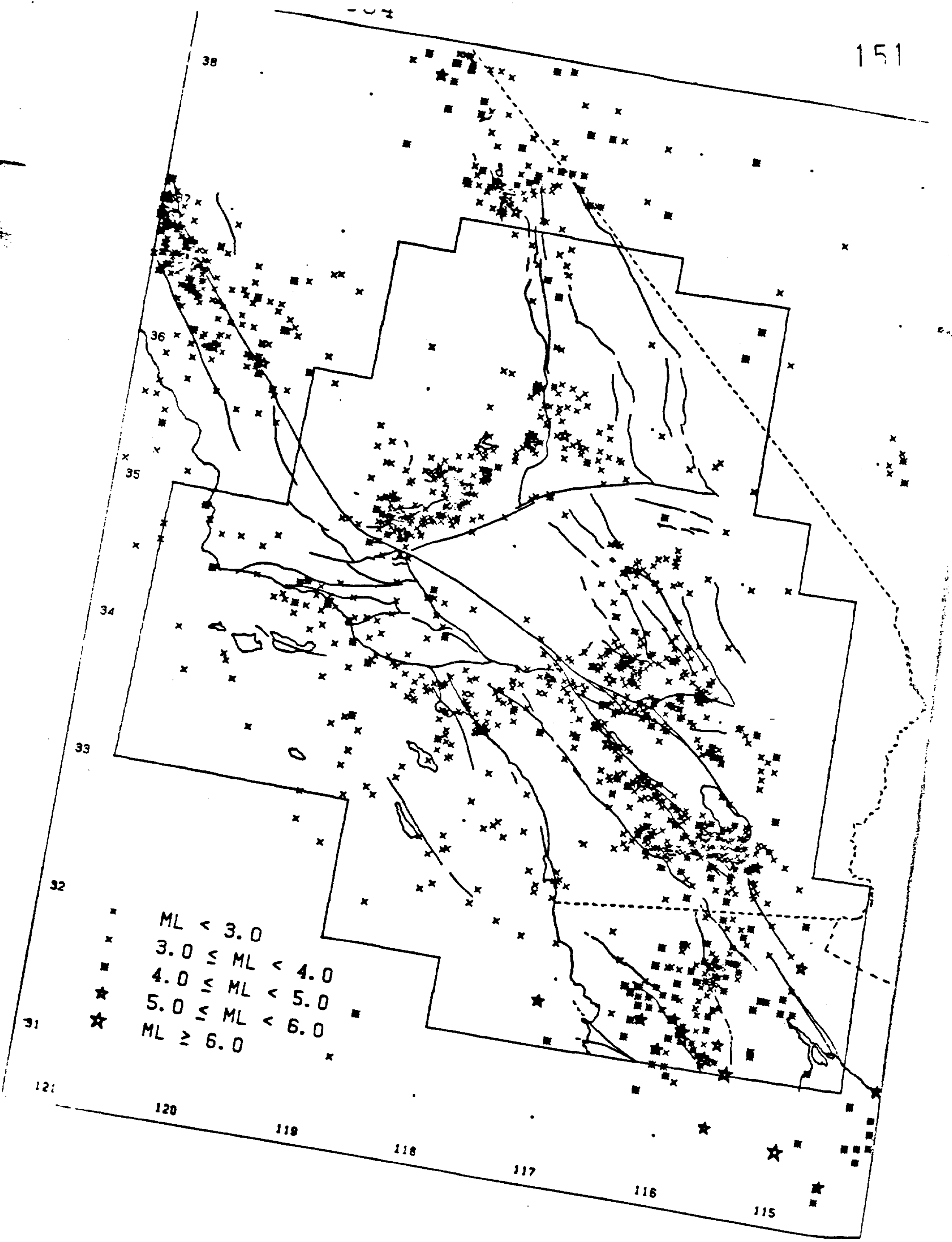
38
36
35
34
33
32
31
121
120
119
118
117
116
115
ML < 3.0
3.0 ≤ ML < 4.0
4.0 ≤ ML < 5.0
5.0 ≤ ML < 6.0
ML ≥ 6.0

1965 - 1974

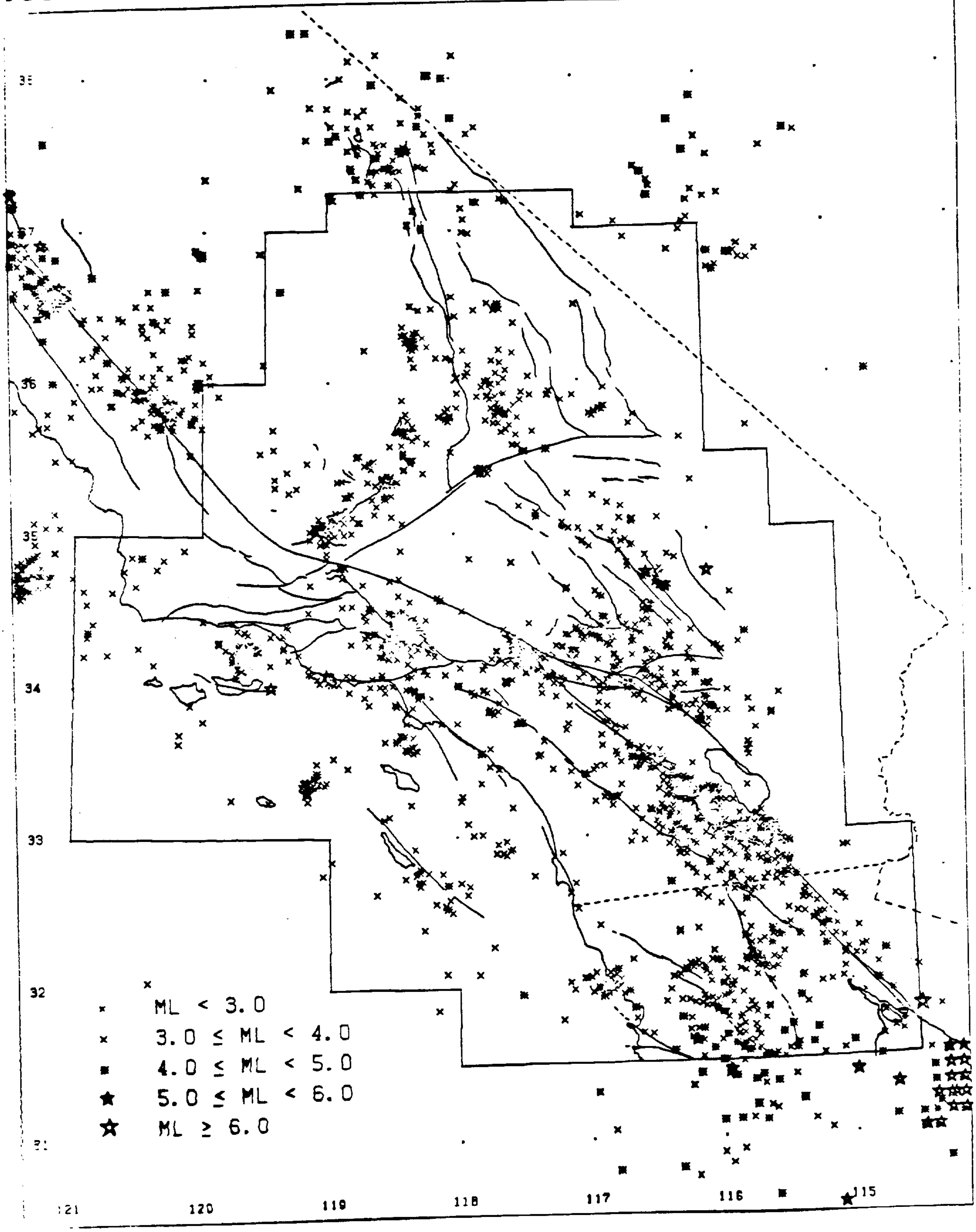
ML < 3.0
3.0 ≤ ML < 4.0
4.0 ≤ ML < 5.0
5.0 ≤ ML < 6.0
ML ≥ 6.0
35
34
33
32
120
119
118
117
116
115